

## Amorphous TiO<sub>2</sub> coated into periodic mesoporous organosilicate channels as a new binary photocatalyst for regeneration of carbonyl compounds from oximes under sunlight irradiation†

Cite this: *Org. Biomol. Chem.*, 2013, **11**, 416

Received 28th September 2012,  
Accepted 12th November 2012

DOI: 10.1039/c2ob26907d

www.rsc.org/obc

Sedigheh Abedi,<sup>a</sup> Babak Karimi,<sup>\*a</sup> Foad Kazemi,<sup>a</sup> Mihnea Bostina<sup>b</sup> and Hojatollah Vali<sup>b</sup>

**A new binary photocatalyst was easily prepared based on incorporation of amorphous titania into the periodic mesoporous organosilicate framework bearing photoresponsive isocyanurate species. The catalyst was found to be highly active in photocatalytic deoxygenation reaction under sunlight irradiation.**

In recent years, the search for environmentally benign chemical processes or methodologies has received increasing attention due to their role in conservation of the global ecosystem.<sup>1</sup> In this regard, owing to the simplified recovery and reusability, the use of heterogeneous catalysis is often favoured for many chemical reactions within both academic and industrial settings.<sup>2</sup> However, in addition to reusability, one of the most important desiderata in the field of sustainable chemistry is to replace the toxic and expensive metal-based catalysts by safer analogs accompanied with employing renewable and more accessible energy sources whilst demonstrating similar or even higher levels of activity. Along this line, heterogeneous photocatalysts comprising semiconductor metal oxides have been recognized as promising tools to attain this goal in organic transformations.<sup>3</sup> Amongst them, TiO<sub>2</sub> has gained considerable attention due to its low cost, high stability under irradiation and environmentally friendliness.<sup>4</sup> However, the major limitation when using TiO<sub>2</sub> as a photocatalyst is its very low selectivity due to the large band gap, which often resulted in a variety of undesired by-products in many applications.<sup>5</sup> Furthermore, most of the studies have been focused on modifying crystalline forms of TiO<sub>2</sub> to obtain a new improved photocatalyst system, as these materials are traditionally

thought to be more suitable for the catalytic applications.<sup>6</sup> It seems that the chemists have largely ignored the intrinsic advantages of amorphous TiO<sub>2</sub>-based photocatalytic systems such as simple preparation process and relatively high surface area leading to high adsorptivity. Nevertheless, to date there have been only a few studies successfully employing amorphous TiO<sub>2</sub> and TiO<sub>2</sub>-based composites in photochemical transformations.<sup>7</sup>

Another interesting approach to improve the photocatalytic performance/selectivity of TiO<sub>2</sub> is the immobilization of a titanium precursor onto a large surface area and inert solid support with a primary objective of achieving more active sites per unit area. In this regard, the use of ordered mesoporous silicas such as MCM-41<sup>8</sup> and SBA-15<sup>9</sup> with large surface area and regular pore size in the range of 2–30 nm is well established in preparing various types of supported titania catalysts.<sup>10</sup> One of the impressive breakthroughs in the area of mesoporous material was the discovery of periodic mesoporous organosilicas (PMOs),<sup>11</sup> which are built from the condensation of bridge organosilane [(R'O)<sub>3</sub>Si–R–Si(OR')<sub>3</sub>]. PMOs have not only better hydrothermal and mechanical stability than ordered mesoporous materials, but also organic groups, R, that are homogeneously distributed throughout the stable silica network. Moreover, incorporation of bridging groups provides a means of precise tuning the surface properties of PMOs to achieve the desired functionality and/or selectivity. However, despite the unique characteristic of PMOs, their impact as the supports in photocatalytic systems has been unexplored to date. Inspired by our successful experience in designing several PMO-supported catalyst systems,<sup>12</sup> we hypothesized that PMOs bearing an appropriate photoresponsive and photoresistance organic group inside their framework might be an attractive or even better matrix than non-functionalized mesoporous silicas in immobilizing amorphous TiO<sub>2</sub>. If this hypothesis could be validated in practice, the approach would offer the possibility of designing an unprecedented family of heterogeneous photocatalysts based on a synergism between integrated organic functional groups located in close

<sup>a</sup>Department of Chemistry, Institute for Advanced Studies in Basic Sciences (IASBS), Gava Zang, Zanjan 45137-66731, Iran. E-mail: karimi@iasbs.ac.ir; Fax: +98-241-4214949; Tel: +98-241-4153225

<sup>b</sup>Anatomy and Cell Biology and Facility for Electron Microscopy Research, McGill University, Montreal, Quebec, H3A 2A7 Canada

†Electronic supplementary information (ESI) available: The experimental details for the preparation of catalysts, recycling results, N<sub>2</sub> absorption-desorption and BJH analyses, IR spectra, TGA, elemental analyses and TEM images of PICS-Ti (45). See DOI: 10.1039/c2ob26907d

proximity of titanium sites on a porous surface. However, the efficiency-selectivity couples and durability of the photocatalyst systems could not only depend on the above-mentioned synergism but they may also strongly rely on the photoresponsive and photoresistance nature of the functionalized organic moieties.

The interesting findings of Tetzlaff and Jenks<sup>13</sup> and Kisch and Mitoraj<sup>14</sup> concerning the outstanding photoresistance and photoresponsive behavior of cyanuric acid stimulated our interest in investigating whether the combination of these photochemical properties and photocatalytic activity of amorphous TiO<sub>2</sub> in the pore structure of PMOs would lead to an improved catalytic performance. To validate this hypothesis, we have chosen a known isocyanurate PMO (PMO-ICS) which can be easily prepared by hydrolysis co-condensation of tris-[3-methoxysilylpropyl]isocyanurate (ICS) and tetraethoxysilane (TEOS) in the presence of pluronic P123 as a structure directing agent under acidic conditions.<sup>15</sup> The surface of the resulting PMO-ICS was then modified by amorphous TiO<sub>2</sub> through a layer-by-layer coating procedure to give PICS-Ti (x).<sup>16</sup> Four catalysts with varying percentage of loaded TiO<sub>2</sub> (25, 35, 45, 55) have been prepared by employing Ti(Oi-Pr)<sub>4</sub> (TTIP) as a titanium precursor and the resulting samples were denoted as PICS-Ti (25), PICS-Ti (35), ICS-Ti (45), PICS-Ti (55), respectively. All PICS-Ti samples were thoroughly characterized by N<sub>2</sub> adsorption-desorption analysis, X-ray diffraction, transmission electron microscopy (TEM) and 3D electron tomography (3D-ET). The structural parameters of the materials are collected in Table 1. As can be clearly seen both BET surface area and average pore diameters decrease upon increasing the amount of TTIP in the coating stage, highlighting the notion that the TiO<sub>2</sub> layer might be indeed well incorporated in the interior of mesochannels of the pristine PMO-ICS.<sup>17</sup> All samples were also found to be amorphous according to high-angle X-ray diffraction, indicating the absence of any crystalline TiO<sub>2</sub> domains. On the other hand, TEM images of materials provided strong evidence that 2D-hexagonal

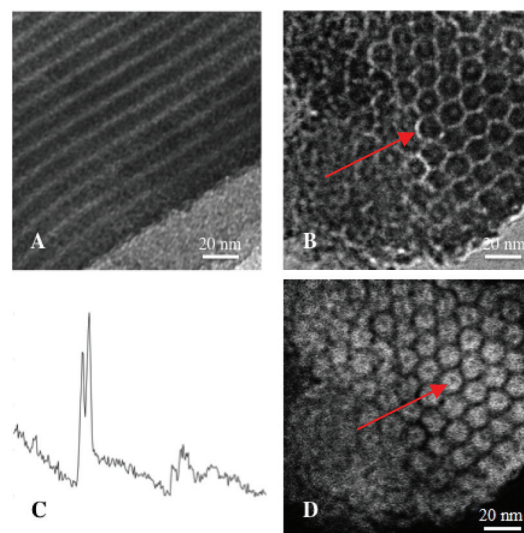


**Fig. 1** Electron microscopy of PICS-Ti (45). (A) Across the 2D-hexagonal channels. (B) An image showing a longitudinal view of the 2D-hexagonal channels, homogeneous presence of TiO<sub>2</sub> in the material in dark mode. The wall of mesochannels can be clearly seen in bright color. (C) EELS spectra of the image presented in B showing the presence of the TiO<sub>2</sub>. (D) EFTEM image of the image in B demonstrating the homogeneous presence of TiO<sub>2</sub> in the material in bright mode. TiO<sub>2</sub> layers are clearly visible.

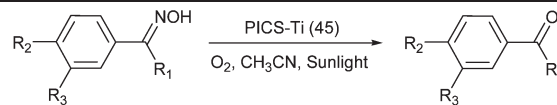
mesostructure of the parent PMO-ICS was retained intact after the coating of titania (Fig. 1). Moreover, both EELS spectra and EFTEM of the materials clearly demonstrate the homogeneous distribution of Ti in the materials (Fig. 1C, 1D).

To gain more insight into the ultrastructure of the TiO<sub>2</sub>-loaded materials, ET and 3D-reconstruction techniques were employed (Fig. S9 in ESI†). These images clearly demonstrate that all ordered arrays of a homogeneous titania thin layer are well associated with the internal surface of mesopores of the PMO-ICS, and there is no separate TiO<sub>2</sub> nano-domain in the materials. Furthermore, 3D-reconstruction images also indicated that no channel blockage has occurred in the PICS-Ti (45) (Fig. S9 in ESI†), which is a very promising feature for application in catalysis. Since our initial goal of this research was to employ mesoporous organosilica/amorphous TiO<sub>2</sub> nanocomposites with varying degree of loaded titania inside their mesochannels in catalysis, we were then very interested to compare the catalytic performance of these nanocomposite materials in photochemical deprotection of oximes as a probe under sunlight irradiation. Despite the fact that lots of methods have been developed for the generation of carbonyl compounds from oximes,<sup>18</sup> the number of energy efficient systems reported in the literature involving TiO<sub>2</sub> are very limited.<sup>19</sup> In the first step of our study, we immediately realized that among the different kinds of TiO<sub>2</sub>-loaded PMO-ICS materials, which had varying degree of TiO<sub>2</sub> content, the catalyst having 45% TiO<sub>2</sub> inside the mesochannels (PICS-Ti (45)) is the most active in the oxidative deprotection of acetophenone oxime using molecular oxygen under sunlight irradiation (Table 1), giving almost quantitative yields of acetophenone.

**Table 1** Structural parameters of PMO-ICS and PICS-Ti with varied Ti loading

Catalyst	$S_{\text{BET}}$ [m <sup>2</sup> g <sup>-1</sup> ]	$D_{\text{BJH}}$ [nm]	$V_{\text{t}}$ [cm <sup>3</sup> g <sup>-1</sup> ]	Acetophenone yield <sup>a</sup> [%]
PMO-ICS	564	6.5	0.804	—
PICS-Ti (25)	445	3.32	0.59	14 <sup>b</sup>
PICS-Ti (35)	443	2.4	0.42	54 <sup>b</sup>
PICS-Ti (45)	400	2.4	0.578	100 <sup>c</sup>
PICS-Ti (55)	307	2.4	0.203	78 <sup>b</sup>
PICS-Ti (45B)	355	2.4	0.485	99 <sup>d</sup>
PICS-Ti (45T)	—	—	—	99 <sup>e</sup>
PMO-Ph-Ti (45)	440	2.2	0.650	70 <sup>f</sup>

<sup>a</sup> GC yield using an internal standard (biphenyl) method unless otherwise stated, reaction condition: oxime (20 mg), catalyst (25 mg), 12 ml dry CH<sub>3</sub>CN, O<sub>2</sub> atmosphere (1 atm.), daily sunlight (10 am–4 pm). <sup>b</sup> Reaction time 10 h. <sup>c</sup> During 2 h. <sup>d</sup> The reaction was performed using the recovered catalyst, PICS-Ti (45R), during 8 h. <sup>e</sup> Thermally treated catalyst PICS-Ti (45T) at 400 °C was employed, reaction time 2 h. <sup>f</sup> The reaction was performed using PMO-Ph-Ti (45) having a 100% phenylene group, reaction time 7 h.

**Table 2** Regeneration of carbonyl compounds from oximes under sunlight irradiation using PICS-Ti (45)


Entry	R <sub>1</sub>	R <sub>2</sub>	R <sub>3</sub>	Time [h]	Yield <sup>a</sup> [%]	Daily temp. range [°C]
1 <sup>b</sup>	Me	H	H	15	6	25–35
2	H	H	H	7	95	29–35
3	H	Cl	H	10	93	27–33
4	H	Me	H	6	97	24–33
5	Me	H	H	2	100	23–32
6 <sup>c</sup>	Me	H	H	4	100	33–39
7	Me	Me	H	1	100	35–39
8	Me	OCH <sub>3</sub>	H	1	100	27–33
9	Me	Cl	H	6	100	26–35
10	Me	H	Br	6	100	22–35
11	Et	H	H	4	100	20–32
12	Ph	H	H	6	100	25–35
13	2-Pyridyl acetophenone oxime			7	100	27–37
14 <sup>d</sup>	Me	H	H	10	82	28–35
15 <sup>e</sup>	Me	H	H	10	7	27–35
16 <sup>f</sup>	Me	H	H	15	2	28–37

<sup>a</sup>GC yield using an internal standard (biphenyl) method unless otherwise stated, reaction condition: oxime (20 mg), catalyst (25 mg), 12 ml dry CH<sub>3</sub>CN, O<sub>2</sub> atmosphere (1 atm.), daily sunlight (10 am–4 pm, sunlight intensity between 80–10 × 10<sup>3</sup> Lux). <sup>b</sup>In the dark. <sup>c</sup>In the presence of 10 mg of the catalyst. <sup>d</sup>25 mg SBA-15 having 45% TiO<sub>2</sub> loading as photocatalyst. <sup>e</sup>With 25 mg of pure amorphous TiO<sub>2</sub> as photocatalyst. <sup>f</sup>Without catalyst.

A survey of reaction media for this photocatalytic reaction revealed that dry CH<sub>3</sub>CN provides the highest product yields and selectivity. On the basis of this encouraging result, we then speculate that this catalyst system might be also useful to accomplish the same transformation for other types of structurally diverse oximes. With optimized reaction conditions in hand, we then proceeded to examine briefly the scope of this photocatalytic deoxygenation reaction.

As summarized in Table 2, various types of aromatic aldoximes and ketoximes were selectively oxidized to their corresponding carbonyl compounds in excellent yields within relatively short reaction times. The reaction of acetophenone oxime in the presence of PICS-Ti (45) in the dark gave only 6% of acetophenone after 15 h, which confirmed that the TiO<sub>2</sub> layer in our catalyst is not acting as a Lewis acid catalyst (Table 2, entry 1). It was also verified that in the absence of a catalyst no reactions occurred in sunlight under the oxygen atmosphere (Table 2, entry 16). The higher activity of ketoximes particularly electron-rich substrates in comparison with aldoximes implies that the difference is possibly due to cationic character of intermediates in deoxygenation reaction.<sup>19b</sup> However, variation in either electronic nature or steric hindrance has little influence on the product yields and selectivity. It is worth mentioning that all reactions have been carried out using as low as 25 mg PICS-Ti (45), which contains just 11 mg of amorphous TiO<sub>2</sub>, in daily ambient temperature and

sunlight intensity ranging 80–100 × 10<sup>3</sup> Lux. To our knowledge there has been no precedent example of using amorphous TiO<sub>2</sub> under such mild reaction as well as optical conditions in the deprotection of oximes. In order to make better comparison, the photocatalytic aerobic oxidation of benzophenone oxime was also tested using PMO-Ph-Ti (45) bearing a 100% phenylene group instead of an isocyanuric group under the same reaction conditions with the same TiO<sub>2</sub> loading as PMO-Ph-Ti (45), gave only 70% acetophenone within 7 hours (Table 1). In a separate experiment the use of mesoporous silica SBA-15 having essentially the same amorphous TiO<sub>2</sub> was shown to afford much inferior results in the deprotection of acetophenone oxime under the described reaction conditions (Table 2, entry 14). Notably, we found that the catalytic performance of amorphous TiO<sub>2</sub> prepared using a known procedure was quite negligible under the same reaction conditions (Table 2, entry 15). These data imply that the high performance of the present photocatalyst system might be most likely originated from the isocyanuric groups embedding inside the silica frameworks.

On the basis of the above observations, we may conclude that the excellent activity and selectivity of PICS-Ti (45) in the described deoxygenation can be correlated to an unprecedentedly reported and unique double synergetic effect of the presence of isocyanuric groups in the pristine PMO-ICS as well as the existing mesoporosity of the support where the titania photoactive sites are located.

We also investigated the recycling PICS-Ti (45) photocatalyst from the reaction mixture of acetophenone oxime. After each run, the catalyst was separated and washed with a mixture of CH<sub>3</sub>CN–MeOH (1 : 1), and dried at 75 °C under air. The catalyst was then successfully reused in five consecutive runs and showed a slight decrease in the catalytic activity after each recycling (Table S2 in ESI†). While the elemental analysis of the catalyst after the first reaction cycle showed that the TiO<sub>2</sub> content reduced to 36%, the total organic content remained unchanged (Table S3 in ESI†). On the other hand, TEM images of the recovered catalyst also displayed a few inhomogeneity (segregation) in the supported TiO<sub>2</sub> domains (Fig. S8 in ESI†). N<sub>2</sub> sorption analysis of the recovered catalyst also confirms that the material mostly retains its mesostructure, whereas both BET surface area and BJH pore size have been considerably reduced. Consequently, the small decrease of catalytic activity of PICS-Ti (45) seems to be a result of either leaching of titanium species during the reaction or TiO<sub>2</sub> segregation.

The authors acknowledge IASBS Research Councils for support of this work.

## Notes and references

- 1 P. T. Anastas and M. M. Kirchhoff, *Acc. Chem. Res.*, 2002, **35**, 686.
- 2 (a) J. H. Clark, *Acc. Chem. Res.*, 2002, **35**, 791; (b) J. M. Thomas, J. C. Hernandez-Garrido and R. G. Bell, *Top. Catal.*, 2009, **52**, 1630.

- 3 G. Palmisano, V. Augugliaro, M. Pagliaro and L. Palmisano, *Chem. Commun.*, 2007, 3425.
- 4 A. Linsebigler, G. Lu and J. T. Yates, *Chem. Rev.*, 1995, **95**, 735.
- 5 G. Palmisano, E. García-López, G. Marci, V. Loddo, S. Yurdakal, V. Augugliaro and L. Palmisano, *Chem. Commun.*, 2010, **46**, 7074.
- 6 (a) R. Asahi, T. Morikawa, T. Ohwaki, K. Aoki and Y. Taga, *Science*, 2001, **293**, 269; (b) S. U. M. Khan, M. Al-Shahry and W. B. Ingler Jr., *Science*, 2002, **297**, 2243; (c) S. S. Soni, M. J. Henderson, J. Bardeau and A. Gibaud, *Adv. Mater.*, 2008, **20**, 1493; (d) D. Mitoraj and H. Kisch, *Chem.–Eur. J.*, 2010, **16**, 261 and many other references.
- 7 L. Zang, W. Macyk, C. Lange, W. F. Maier, C. Antonius, D. Meissner and H. Kisch, *Chem.–Eur. J.*, 2000, **6**, 379.
- 8 (a) C. T. Kresge, M. E. Leonowicz, W. J. Roth, J. C. Vartuli and J. S. Beck, *Nature*, 1992, **359**, 710; (b) J. S. Beck, J. C. Vartuli, W. J. Roth, M. E. Leonowicz and C. T. Kresge, *J. Am. Chem. Soc.*, 1992, **114**, 10834.
- 9 (a) D. Zhao, J. Feng, Q. Huo, N. Melosh, G. H. Fredrickson, B. F. Chmelka and G. D. Stucky, *Science*, 1998, **279**, 548; (b) D. Zhao, Q. Huo, J. Feng, B. F. Chmelka and G. D. Stucky, *J. Am. Chem. Soc.*, 1998, **120**, 6024.
- 10 (a) F. Bérubé, A. Khadhraoui, M. T. Janicke, F. Kleitz and S. Kaliaguine, *Ind. Eng. Chem. Res.*, 2010, **49**, 6977; (b) J. N. Primera-Pedrozo, B. D. Torres-Cosme, M. E. Clardy, M. E. Rivera-Ramos and A. J. Hernández-Maldonado, *Ind. Eng. Chem. Res.*, 2010, **49**, 7515, and many other references.
- 11 (a) T. Asefa, N. Coombs, M. J. MacLachlan and G. A. Ozin, *Nature*, 1999, **402**, 867; (b) S. Inagaki, S. Guan, Y. Fukushima, T. Ohsuna and O. Terasaki, *J. Am. Chem. Soc.*, 1999, **121**, 9611; (c) B. J. Melde, B. T. Holland, C. F. Blanford and A. Stein, *Chem. Mater.*, 1999, **11**, 3302.
- 12 (a) B. Karimi, D. Elhamifar, J. H. Clark and A. J. Hunt, *Chem.–Eur. J.*, 2010, **16**, 8047; (b) B. Karimi, D. Elhamifar, J. H. Clark and A. J. Hunt, *Org. Biomol. Chem.*, 2011, **9**, 7420; (c) B. Karimi and F. Kabiri Esfahani, *Chem. Commun.*, 2011, **47**, 10452; (d) B. Karimi, H. M. Mirzaei and A. Mobaraki, *Catal. Sci. Technol.*, 2012, **2**, 828; (e) B. Karimi and F. Kabiri Esfahani, *Adv. Synth. Catal.*, 2012, **354**, 1319.
- 13 T. A. Tetzlaff and W. S. Jenks, *Org. Lett.*, 1999, **1**, 463.
- 14 H. Kisch and D. Mitoraj, *Angew. Chem., Int. Ed.*, 2008, **47**, 9975.
- 15 M. Jaroniec and O. Olkhoviyk, *J. Am. Chem. Soc.*, 2005, **127**, 60.
- 16 S. Dai, W. Yan, M. Mahurin and S. H. Overbury, *Chem. Mater.*, 2005, **17**, 1923.
- 17 See the ESI† for surface analyses diagrams.
- 18 (a) D. H. R. Barton, J. M. Beaton, L. E. Geller and M. M. Pechet, *J. Am. Chem. Soc.*, 1961, **83**, 4076; (b) D. H. R. Barton and J. M. Beaton, *J. Am. Chem. Soc.*, 1961, **83**, 4083; (c) R. S. Varma, *Green Chem.*, 1999, **1**, 43; (d) W. Chrisman, M. J. Blankinship, B. Taylor and C. E. Harris, *Tetrahedron Lett.*, 2001, **42**, 4775; (e) A. Khazaei, R. G. Vaghei and M. Tajbakhsh, *Tetrahedron Lett.*, 2001, **42**, 5099.
- 19 (a) C. Saravanseli, N. Somasundaram, S. Vijaikumar and C. Srinivasan, *Photochem. Photobiol. Sci.*, 2002, **1**, 607; (b) M. Swaminathan, K. Muthu, K. Selvam and B. Krishnakumar, *Appl. Catal., A*, 2009, **358**, 259.